THE OHIO STATE UNIVERSITY

CALCULATION OF THE EFFECTS OF ICE ON THE BACKSCATTER OF A GROUND PLANE

K.M. Lambert
L. Peters, Jr.

The Ohio State University
ElectroScience Laboratory

Department of Electrical Engineering
Columbus, Ohio 43212

Technical Report 720964-1
Grant NAG3-913
September 1988

NATIONAL AERONAUTICS AND SPACE ADMINISTRATION
Lewis Research Center
21000 Brookpark Rd.
Cleveland, Ohio 44135

NOTICES

When Government drawings, specifications, or other data are used for any purpose other than in connection with a definitely related Government procurement operation, the United States Government thereby incurs no responsibility nor any obligation whatsoever, and the fact that the Government may have formulated, furnished, or in any way supplied the said drawings, specifications, or other data, is not to be regarded by implication or otherwise as in any manner licensing the holder or any other person or corporation, or conveying any rights or permission to manufacture, use, or sell any patented invention that may in any way be related thereto.

50272-101

REPORT DOCUMENTATION PAGE	1. REPORT NO.	2.	3. Recipient's Accession No

4. Title and Subtitle

CALCULATION OF THE EFFECTS OF ICE ON THE BACKSCATTER OF A GROUND PLANE

5. Report Date: September 1988

6.

7. Author(s)

K.M. Lambert and L. Peters, Jr.

8. Performing Organization Rept. No: 720964-1

9. Performing Organization Name and Address

The Ohio State University
ElectroScience Laboratory
1320 Kinnear Road
Columbus, Ohio 43212

10. Project/Task/Work Unit No.

11. Contract(C) or Grant(G) No.

(C)

(G) NAG3-913

12. Sponsoring Organization Name and Address

National Aeronautics and Space Administration
Lewis Research Center
21000 Brookpark Rd.
Cleveland, Ohio 44135

13. Type of Report & Period Covered: Technical

14.

15. Supplementary Notes

16. Abstract (Limit: 200 words)

This report describes a technique for examining the effect of a rough ice layer on the backscatter of a ground plane. The technique is applied to the special case of a rough ice layer that is periodic in space. By assuming that the roughness is periodic, the backscatter of the ground plane can be found from the backscatter of a single period. Backscatter calculations are presented for a single period in which the thickness of the ice layer has a Gaussian shape.

17. Document Analysis a. Descriptors

b. Identifiers/Open-Ended Terms

c. COSATI Field/Group

18. Availability Statement	19. Security Class (This Report): Unclassified	21. No. of Pages: 50
	20. Security Class (This Page): Unclassified	22. Price

(See ANSI-Z39.18) See Instructions on Reverse

OPTIONAL FORM 272 (4-77)
(Formerly NTIS-35)
Department of Commerce

TABLE OF CONTENTS

LIST OF FIGURES

I. INTRODUCTION

This report presents some calculated results of the effects that pure water ice has on the backscatter pattern of a perfectly conducting ground plane. Pure water ice has very small losses and therefore a uniform ice layer has little effect on the backscatter of the ground plane. This would not be the case for other geometries since a curved ice surface would introduce a lens mechanism. On the other hand, a rough ice layer, where the thickness of the ice varies as a function of a spatial coordinate, can significantly alter the manner in which the ground plane reflects electromagnetic energy. This report investigates the changes in the backscatter pattern which are due to one type of ice roughness.

The analysis of the backscatter from a ground plane covered with an ice layer of non-uniform thickness is similar to the analysis of dielectric multilayers with layer thickness distortions [1]. This analysis is based on a Physical Optics approximation to the reflected field. Briefly, this approximation treats each point on the rough ice surface as if the point were on an infinite tangent plane to that point. This allows the rough surface to be treated as a uniform ice layer, at that point, and the reflected field can be found for that point. An aperture is set up around the ice covered ground plane, and the reflected fields from each point are taken as aperture fields. The reflected field from the entire structure is then produced from an aperture integration using a free space Green's function. Note that this study does not include the influence of surface waves. This

analysis technique is described in mathematical detail in Section II along with a discussion of the net result.

Examples of the results generated by the technique are given in Section III. The ice surface roughness is represented by a Gaussian function and the results for various amplitudes of the Gaussian function are given. Section IV summarizes the technique and the limitations which should be considered when using it.

II. DERIVATION OF THE BACKSCATTERED FIELD

A. Introduction

This section is concerned with presenting the mathematical derivation of the backscattered field from a layer of ice of non-uniform thickness on a ground plane. The ice may be considered to be the first layer of a two layer dielectric multilayer structure that is backed by a conducting plane. This model of the ice covered ground plane is depicted in Figure 2.1. In the figure, Layer 1 is a uniform ice layer, having constitutive parameters ε_1, μ_1. Layer 1 is bounded on one side by the ground plane and on the other side by Layer 2. Layer 2 is simply a free space layer which is included in order that the $z=0$ plane can be used as the aperture plane. The ice covered ground plane has a rectangular area, $L_x L_y$, and the ground plane is centered with respect to the x and y axes.

A rough ice layer on a ground plane may be modeled as a two-layer dielectric multilayer structure with a thickness distortion of the layers. An example of this idea is shown in Figure 2.2. As before, Layer 1 is the ice layer and Layer 2 is simply free space. The

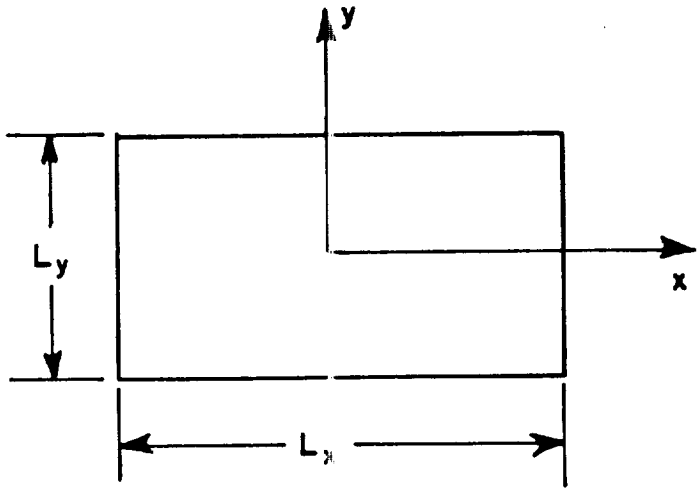

(a)

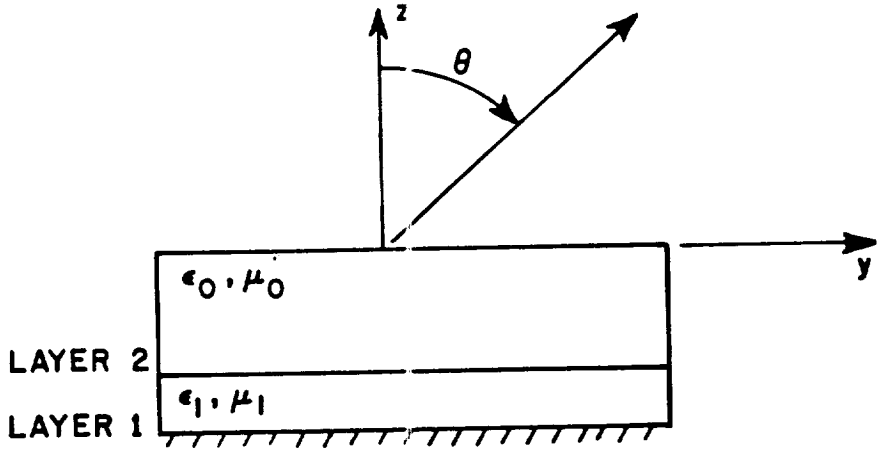

(b)

Figure 2.1. Geometry of a ground plane with a uniform layer of ice.

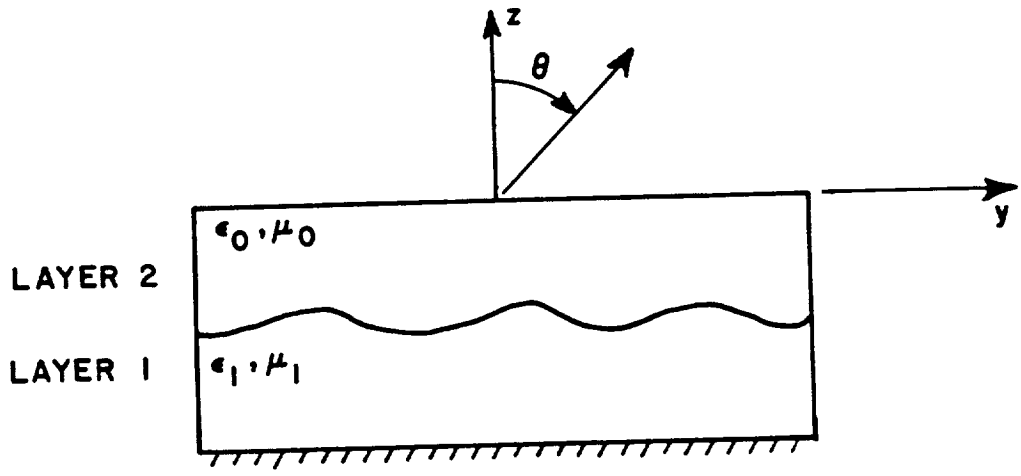

Figure 2.2. Ground plane covered with a non-uniform thickness of ice, modeled as a two-layer multilayer with layer thickness distortions.

presence of Layer 2 allows the aperture plane to remain as the z=0 plane, even with the rough ice present. The goal of this study is to determine the effect that the roughness of the ice has on the backscatter of the ground plane.

Although not necessary, this report will investigate the backscattered field in the $\hat{y}$-$\hat{z}$(ϕ=90°) plane, where it is a maximum. This is done mainly to simplify the discussion of the results. It also prohibits the presentation of the examples from getting excessive. The extension to other ϕ-planes is straightforward and can be done if necessary.

During the mathematical development of the backscattered field, the ice covered ground plane will be treated as a two layer dielectric

multilayer backed by a ground plane. When the ice has a uniform thickness, this multilayer is a planar multilayer since the boundaries between the layers form planes. A rough ice surface will be treated as a thickness distortion in the layers of the multilayer. A plane wave is assumed to be incident on the two layer multilayer from the direction indicated by (θ) in Figure 2.2, and the backscattered field is to be determined. The polarization of the incident wave separates the analysis into two cases. A TE wave or perpendicularly polarized wave (to the incidence plane) will be treated first, after which will follow the case of TM or parallel polarized incidence.

B. TE Case

For the TE case, the incident electric field can be written as,

$$E_x^i = E_o e^{jky\sin\theta} e^{jkz\cos\theta} , \tag{2.1}$$

where $k=\frac{2\pi}{\lambda}$ is the free space wave number. Under the Physical Optics approximation described in the introduction, a point (x,y) on a distorted multilayer will cause a reflected plane wave,

$$E_r^x = R(x,y,\theta)\, E_o e^{jky\sin\theta}\, e^{-jkz\cos\theta} \tag{2.2}$$

where $R(x,y,\theta)$ is the reflection coefficient of a planar multilayer having the same geometry of the distorted multilayer, at the point (x,y), for an angle of incidence, (θ). This expression for the reflected field should be a reasonable approximation for the true field

provided that the radius of curvature of the distortion at the point (x,y) is sufficiently large.

As mentioned earlier, the z=0 plane is chosen to be the aperture plane. The reflected field given by Equation (2.2) can be used to form the equivalent magnetic current, $\bar{M}$, in the aperture. The magnetic current is found from,

$$\bar{M} = 2\,\bar{E}_a \times \hat{n} \tag{2.3}$$

where $\bar{E}_a$ is the aperture field. Combining Equations (2.2) and (2.3), and noting that $\hat{n} \doteq \hat{z}$ for large radii of curvature,

$$\bar{M} = \begin{cases} -2\,E_o R(x,y,\theta) e^{jky\sin\theta}\,\hat{y} & |x| \le \frac{L_x}{2}\,,\ |y| \le \frac{L_y}{2} \\ 0 & |x| > \frac{L_x}{2}\,,\ |y| > \frac{L_y}{2} \end{cases} \tag{2.4}$$

which shows the assumption of zero aperture field outside of the multilayer. The equivalent magnetic current can be integrated with the free space Green's function to produce the electric vector potential $\bar{F}$ [2]

$$\bar{F} = \frac{e^{-jkr}}{4\pi r} \iint \bar{M}(r')\, e^{jkf\cdot r'}\, ds' \tag{2.5}$$

where f is the radial unit vector,

r′ is the source location,

r is the distance to a far field point,

and the integration is over the entire aperture.

Using Equation (2.4) in Equation (2.5) produces

$$\bar{F} = \frac{-e^{-jkr}}{2\pi r} E_o \int_{-L_x/2}^{L_x/2} \int_{-L_y/2}^{L_y/2} R(x,y,\theta)\, e^{j2ky\sin\theta}\, dxdy\, \hat{y} \qquad (2.6)$$

which is the result from considering the ϕ=90° plane and for considering backscatter. Since

$$\hat{y} = \hat{r}\sin\theta\sin\phi + \hat{\theta}\sin\theta\sin\phi + \hat{\phi}\cos\phi$$

in the ϕ=90° plane,

$$\hat{y} = \hat{r}\sin\theta + \hat{\theta}\cos\theta \quad . \qquad (2.7)$$

Finally, from [2],

$$E_\theta = -jkF_\phi$$

$$E_\phi = jkF_\theta$$

which, from using Equations (2.6) and (2.7), results in the backscattered field,

$$E_\phi = \frac{-e^{-jkr}}{2\pi r} jkE_o\cos\theta \int_{-L_x/2}^{L_x/2} \int_{-L_y/2}^{L_y/2} R(x,y,\theta)e^{j2ky\sin\theta}\, dxdy \quad (2.8)$$

and

$$E_\theta = 0 \ . \quad (2.9)$$

Obviously, to find the backscattered field, the integral,

$$Q(\theta) = \int_{-L_x/2}^{L_x/2} \int_{-L_y/2}^{L_y/2} R(x,y,\theta)e^{j2ky\sin\theta}\, dxdy \quad (2.10)$$

must be solved. This can be done numerically provided that the planar multilayer reflection coefficients, $R(x,y,\theta)$, can be found. To find these, use has been made of the recursive technique of Richmond [3]. With this technique, the Physical Optics approximation and Equation (2.8), the backscattered field of many types of ice layer distortions can be found.

It is possible to further investigate the effects of ice layer distortions by choosing to study a particular type of distortion. For this report, it is of interest to examine the effects of a distortion that is periodic in space. To further simplify this analysis, distortions which are a function of a single coordinate only will be considered. Hence, the reflection coefficient can be written as,

$$R(x,y,\theta) = R(y,\theta) = R(y+n\Lambda,\theta) \quad (2.11)$$

where n is an integer and Λ is the spatial period of the distortion.

Further, let the length of the ground plane, in the y direction, be an integral number of spatial wavelengths,

$$L_y = M\Lambda \quad . \tag{2.12}$$

Using Equation (2.11) in Equation (2.10), it can be seen that the integral takes the form

$$Q(\theta) = L_x \int_{-L_y/2}^{L_y/2} R(y,\theta)\, e^{j2ky\sin\theta}\, dy \quad . \tag{2.13}$$

This integral can be written as a summation over each period,

$$Q(\theta) = L_x \sum_n \int_{n\Lambda-\Lambda/2}^{n\Lambda+\Lambda/2} R(y,\theta)\, e^{j2ky\sin\theta}\, dy \tag{2.14}$$

and the summation is carried over all of the periods.

Making the variable transformation,

$$\tau + n\Lambda = y \tag{2.15}$$

and recalling Equation (2.11), Equation (2.14) becomes,

$$Q(\theta) = L_x \sum_n \int_{-\Lambda/2}^{\Lambda/2} R(\tau,\theta)\, e^{j2k\sin\theta(\tau+n\Lambda)}\, d\tau \ . \qquad (2.16)$$

Separating the exponential terms leaves the integral independent of the summation,

$$Q(\theta) = L_x \left[\int_{-\Lambda/2}^{\Lambda/2} R(\tau,\theta) e^{j2k\tau\sin\theta}\, d\tau\right] \sum_n e^{j2kn\Lambda\sin\theta} \ . \qquad (2.17)$$

Using Equation (2.17), the backscattered field for a distortion that is periodic in y can be written as,

$$E_\phi = \frac{-e^{-jkr}}{2\pi r}\, jkE_o\cos\theta\, L_x \left[\int_{-\Lambda/2}^{\Lambda/2} R(y,\theta) e^{j2ky\sin\theta}\, dy\right] \sum_n e^{j2kn\Lambda\sin\theta} \ . \qquad (2.18)$$

Note that written in this form, it is evident that the periodically distorted ice layer may be interpreted as an array. The elements of the array are the individual periods of the distorted ice layer. The response of a single period; or element in the array, is represented by the integral in Equation (2.18). The summation in that equation accounts for the phasing differences between the periods or elements in the array. In antenna theory, this term is called the array factor. The array factor is a geometric series and it can be shown to sum to [4]

$$AF = \sum_{n} e^{j2kn\Lambda\sin\theta} = \frac{\sin\left(\frac{u}{2} M\right)}{\sin\left(\frac{u}{2}\right)} \tag{2.19}$$

where $u=2k\Lambda\sin\theta$, and again, M is the total number of periods. This array factor has a maximum value of M and can thus be normalized by writing

$$AF = M \left[\frac{\sin\left(\frac{u}{2} M\right)}{M \sin\left(\frac{u}{2}\right)}\right] \tag{2.20}$$

where the term in the brackets is called the normalized array factor.

Using Equation (2.20) in Equation (2.18), the backscattered field can be written as,

$$E_{\phi} = \frac{-e^{-jkr}}{2\pi r} jkE_o \cos\theta \, L_x M \left[\frac{\sin\left(\frac{u}{2} M\right)}{M \sin\left(\frac{u}{2}\right)}\right] \int_{-\Lambda/2}^{\Lambda/2} R(y,\theta) \, e^{j2ky\sin\theta} dy \, . \tag{2.21}$$

The echo area or radar cross section of the ice covered ground plane, given by,

$$\sigma = 4\pi r^2 \frac{|E_{\phi}|^2}{|E_o|^2} \tag{2.22}$$

would be

$$\sigma = \frac{k^2\cos^2\theta}{\pi}(L_x M)^2 \left[\frac{\sin\left(\frac{u}{2} M\right)}{M \sin\left(\frac{u}{2}\right)}\right]^2 \left|\int_{-\Lambda/2}^{\Lambda/2} R(y,\theta)\, e^{j2ky\sin\theta} dy\right|^2 . \qquad (2.23)$$

This result can be checked by considering the case of a perfect conductor only, $R(y)=-1$, of length $L_y=M\Lambda$. Using the substitution, $\Lambda t=y$, Equation (2.23) can be written as,

$$\sigma = \frac{k^2\cos^2\theta}{\pi}(L_x M\Lambda)^2 \left[\frac{\sin\left(\frac{u}{2} M\right)}{M \sin\left(\frac{u}{2}\right)}\right]^2 \left|\int_{-1/2}^{1/2} e^{jut} dt\right|^2 . \qquad (2.24)$$

The integral produces the well known function,

$$\int_{-1/2}^{1/2} e^{jut} dt = \frac{\sin\left(\frac{u}{2}\right)}{\left(\frac{u}{2}\right)}$$

and thus Equation (2.24) becomes

$$\sigma = \frac{k^2\cos^2\theta}{\pi} (L_x M\Lambda)^2 \left[\frac{\sin\left(\frac{u}{2} M\right)}{\left(\frac{u}{2} M\right)}\right]^2$$

or

$$\sigma = \frac{k^2\cos^2\theta}{\pi} (L_x L_y)^2 \left[\frac{\sin(kL_y\sin\theta)}{(kL_y\sin\theta)}\right]^2 \qquad (2.25)$$

which is the Physical Optics backscatter in the $\phi=90°$ plane of a perfectly conducting plate.

In order to gain some information about the effect of the roughness of the ice alone, it is possible to subtract the backscattered field of the ground plane with a uniform thickness of ice, from the backscattered field of the ground plane with the rough ice layer. Returning to Equation (2.21), this action produces the equation,

$$\Delta E = \frac{-e^{-jkr}}{2\pi r} jkE_o \cos\theta \, L_x M \left[\frac{\sin\left(\frac{u}{2} M\right)}{M \sin\left(\frac{u}{2}\right)}\right] \int_{-\Lambda/2}^{\Lambda/2} \left[R(y,\theta)-R_o(\theta)\right] e^{j2ky\sin\theta} dy \tag{2.26}$$

where $R_o(\theta)$ is the reflection coefficient of the ground plane with the uniform thickness of ice. The thickness of the uniform layer is chosen to be equal to the thickness of the rough layer at the ends of the period ($y=\pm\Lambda/2$). The radar cross section, due to the ice layer distortions alone is then,

$$\Delta\sigma(\theta) = \frac{k^2\cos^2\theta}{\pi}(L_x M)^2 \left[\frac{\sin\left(\frac{u}{2} M\right)}{M \sin\left(\frac{u}{2}\right)}\right]^2 \left| \int_{-\Lambda/2}^{\Lambda/2} \left[R(y,\theta)-R_o(\theta)\right] e^{j2ky\sin\theta} dy \right|^2 . \tag{2.27}$$

In order to consider the effect of a single period alone, assume the multilayer is of unit length in the x direction. Then

$$\Delta\sigma(\theta) = \frac{k^2\cos^2\theta}{\pi} M^2 \left[\frac{\sin\left(\frac{u}{2} M\right)}{M \sin\left(\frac{u}{2}\right)}\right]^2 \left| \int_{-\Lambda/2}^{\Lambda/2} \left[R(y,\theta)-R_o(\theta)\right] e^{j2ky\sin\theta} dy \right|^2 . \tag{2.28}$$

To eliminate the effect of all the periods, divide each side by the array factor,

$$\sigma_p(\theta) = \frac{\Delta\sigma(\theta)}{M^2\left[\frac{\sin\left(\frac{u}{2}M\right)}{M\sin(u/2)}\right]} = \frac{k^2\cos^2\theta}{\pi}\left|\int_{-\Lambda/2}^{\Lambda/2}\left[R(y,\theta)-R_o(\theta)\right]e^{j2ky\sin\theta}dy\right|^2 . \tag{2.29}$$

This equation represents the radar cross section which is due to a single period of the ice roughness. This form is the most useful for this type of study, for it allows just the roughness itself to be studied. Note that the action of isolating a single period of an array of scatterers has introduced artificial edges on the individual scatterer (the ends of the period), that do not appear in the total scatterer. The subtraction aids in an attempt to remove the effects of the edge, by eliminating the first order diffraction of the edges. However, because of the nature of $R(y,\theta)$, there will be higher order diffraction, such as slope diffraction, that is not removed by the subtraction. So although this technique can provide useful information, the limitations stated here must be considered when interpreting the results.

Equation (2.29) also eliminates the need to specify the size of the ground plane. All that is required is the length of the period, Λ, the constitutive parameters of the ice, and a function representing the distortion. Once the radar cross section of a single period is known,

the result can be simply extended to a ground plane of any size. With σ_p known, and knowing that there are M periods of distortion in y,

$$\Delta\sigma(\theta) = \sigma_p(\theta)\, M^2 \left[\frac{\sin\left(\frac{u}{2} M\right)}{M \sin\left(\frac{u}{2}\right)}\right]^2 \left(\frac{L_x}{1}\right)^2 \tag{2.30}$$

where the last term scales the result to any length in the x direction.

Equation (2.29) is the result that has been sought by this study. Examples using this equation will be given in Section III; however, first it will be shown that a similar result may be obtained for TM wave incidence.

C. TM Case

The derivation for TM wave incidence is similar to that followed in the previous section. Here, the incident magnetic field is assumed to be

$$H_x^i = \frac{E_o}{\eta} e^{jky\sin\theta}\, e^{jkz\cos\theta} \tag{2.31}$$

where η is the impedance of free space. The ground plane and ice layer causes the reflected field,

$$H_x^r = R(x,y,\theta)\, \frac{E_o}{\eta} e^{jky\sin\theta}\, e^{-jkz\cos\theta} \tag{2.32}$$

where $R(x,y,\theta)$ is the reflection coefficient, using the Physical Optics approximation, for TM wave incidence. For this case, the equivalent electric currents

$$\bar{J} = 2\hat{n} \times \bar{H}_a \tag{2.33}$$

are found in the aperture,

$$\bar{J} = \begin{cases} 2\frac{E_o}{\eta} R(x,y,\theta) e^{jky\sin\theta}\, \hat{y} & |x| \le \frac{L_x}{2} \quad |y| \le \frac{L_y}{2} \\ 0 & |x| > \frac{L_x}{2} \quad |y| > \frac{L_y}{2} \end{cases} . \tag{2.34}$$

Knowing the equivalent currents, the magnetic vector potential, $\bar{A}$ [2], can be found,

$$\bar{A} = \frac{e^{-jkr}}{4\pi r} \iint \bar{J}(r') e^{jkf\cdot r'} ds'\, \hat{y} \quad , \tag{2.35}$$

from which the backscattered field is obtained by using [2],

$$E_\theta = -j\omega\mu\, A_\theta$$

$$E_\phi = -j\omega\mu\, A_\phi \, . \tag{2.36}$$

Substituting the currents into Equation (2.35), and using Equation (2.36), the backscattered field in the ϕ=90° plane, for TM wave incidence is,

$$E_\theta = \frac{-e^{-jkr}}{2\pi r} jkE_o\cos\theta \int_{-L_x/2}^{L_x/2} \int_{-L_y/2}^{L_y/2} R(x,y,\theta)\, e^{j2ky\sin\theta} dxdy \qquad (2.38)$$

and

$$E_\phi = 0 \quad . \qquad (2.39)$$

Note that E_θ for TM incidence has the identical form that E_ϕ had for TE incidence. The only difference is in the calculated value of the reflection coefficient, since it will be different for the two polarizations.

Because of the similarity of the two expressions, the results of the previous section can be applied here. Assuming periodic distortions in y and no distortions in x as before, the radar cross section of the ice covered ground plane will be

$$\sigma(\theta) = \frac{k^2\cos^2\theta}{\pi} (L_x M)^2 \left[\frac{\sin\left(\frac{u}{2} M\right)}{M \sin\left(\frac{u}{2}\right)}\right]^2 \left|\int_{-\Lambda/2}^{\Lambda/2} R(y,\theta) e^{j2ky\sin\theta} dy\right|^2 \qquad (2.40)$$

where $u=2k\Lambda\sin\theta$ as before.

Similarly, the radar cross section, due to the distortions alone, is

$$\Delta\sigma(\theta) = \frac{k^2\cos^2\theta}{\pi}(L_x M)^2\left[\frac{\sin\left(\frac{u}{2}M\right)}{M\sin\left(\frac{u}{2}\right)}\right]^2\left|\int_{-\Lambda/2}^{\Lambda/2}[R(y,\theta)-R_o(\theta)]e^{j2ky\sin\theta}dy\right|^2, \tag{2.41}$$

and the radar cross section, due to a single period is

$$\sigma_p(\theta) = \frac{k^2\cos^2\theta}{\pi}\left|\int_{-\Lambda/2}^{\Lambda/2}[R(y,\theta)-R_o(\theta)]e^{j2ky\sin\theta}dy\right|^2 . \tag{2.42}$$

The examples to be presented in Section III will show the results of ice covered ground planes for both TE and TM wave incidence.

D. Summary

In this section, the backscattered field of a ground plane covered by an ice layer with non-uniform thickness was considered. The problem was approached by treating the structure as a two layer dielectric multilayer with layer thickness distortions and making a Physical Optics approximation to the distorted layers. In effect, this approximation allowed the reflection coefficients of an infinite planar multilayer to be used. The reflection coefficients were used to find the reflected field of the structure, which in turn were used to find equivalent currents in an aperture plane. The equivalent currents were then integrated to find the backscattered field.

The special case of ice layer thickness that is a periodic function of a single coordinate, was considered in detail. It was found that, for this case, a normalized radar cross section could be found for a single period. The complete radar cross section could be found by multiplying by the number of periods, the normalized array factor, and the length in the other coordinate. Studying the radar cross section in this form allows the effect of the roughness alone to be examined, without having to specify the size of the multilayer.

Only ice distortions of the type mentioned were examined in detail. However, note that any distortion function, in an ice layer of finite size, will at least have a period of unity. Thus, this analysis should have sufficient generality to treat any distortion of ice layer thicknesses, provided $\hat{n}=\hat{z}$ at the surface. Also since distortions were taken to be a function of y only, the backscattered field was only derived for the $\hat{y}$-$\hat{z}$ ($\phi=90°$) plane. Although the equations could have been written more generally, this plane will contain the maximum effect for the type of distortions considered.

The backscattered field was derived for both TE and TM wave incidence. The field for both polarizations was found to have the same form and thus the interpretation is the same. Backscatter from arbitrary polarization of the incident wave can be constructed from these two results.

III. EXAMPLES

A. Introduction

In this chapter, the analysis of the previous section will be applied to several examples of ground planes covered by ice. A Gaussian function will be used to describe the roughness of the ice layer. The examples will demonstrate the effect of the ice roughness as the amplitude and shape of the Gaussian function is varied. Note that physically this represents the thickness variation of the ice layer. The examples will provide plots of the normalized radar cross section of a single period of the distortion function given by Equation (2.29) or Equation (2.42). To extend the results to an actual ice covered ground plane, the terms shown in Equation (2.30) must be included.

One of these terms, the normalized array factor, modifies the angular dependence of the backscatter. For this reason, the section will begin with a review of the array factor and examine what it implies to the backscatter pattern. The examples will be presented after that review.

B. The Array Factor

A discussion of array factors is included in most antenna texts. The array factor, which appears in the backscattered field expression, is a result of the assumption that the distortions in the layer thickness of the multilayer are periodic. The fact that it does appear allows the backscattered field to be interpreted as coming from an array of scatterers. These scatterers, when viewed from the

backscatter direction, appear to be uniformly illuminated, and thus, the normalized array factor,

$$AF = \frac{\sin\left(\frac{u}{2} M\right)}{M \sin\left(\frac{u}{2}\right)} \tag{3.1}$$

is of the same form as the array factor for an M element, uniformly excited, equally spaced array antenna. The difference between the scattering and the antenna is in the interpretation of u. For the antenna, u would be given by,

$$u = kd\sin\theta \tag{3.2}$$

where d is the element spacing. In the backscattering problem,

$$u = 2k\Lambda\sin\theta \tag{3.3}$$

where Λ is the size of the spatial period of the distortion. An extra factor of two appears in Equation (3.3) because for backscatter, the array factor must take into account the relative phase difference between scatterers in the incident field in addition to the relative phase difference between the fields reflected by the scatterers. In an array antenna, there is only the phase difference between the fields radiated by the elements. The net result of this factor of two is that in the scattering problem, the visible region of the array factor is

twice as large as that of an array antenna. This will be further demonstrated shortly.

The array factor shown in Equation (3.1) is periodic, as a function of u, with a period of 2π. It attains a maximum value at $u=2\pi$, where n is an integer. An example of the array factor, for M=3, is shown in Figure 3.1. Other properties of this array factor, as listed in [4] are as follows:

1. As M increases, the width of the main lobe narrows.
2. As M increases, there are more minor lobes in one period of the array factor. The total number of lobes in one period is M-1, with one main lobe and M-2 minor lobes.
3. The width of the main lobe, in u-space, is $4\pi/M$ and the width of the minor lobes are $2\pi/M$.
4. The minor lobe levels decrease with increasing M. As M gets large, the peak minor lobe level approaches the peak minor lobe level of the sin(u)/u function, -13.3 dB.
5. The magnitude of the array factor is symmetric about $u=\pi$.

These properties may be observed by examining graphs of the array factor for different values of M. Figure 3.2 shows the array factor for M=5, Figure 3.3 is M=10, and Figure 3.4 is M=100. Kraus [5] provides a more extensive set of array factor plots.

The array factor is transformed to real space by Equation (3.3). How much of the array factor pattern, or how many periods of it appear in real space, depends on the value of Λ. Note that since the maximum value of $\sin\theta$ is unity, the boundary of real space is given by,

$$u_m = 2k\Lambda = 4\pi \frac{\Lambda}{\lambda} \quad , \tag{3.4}$$

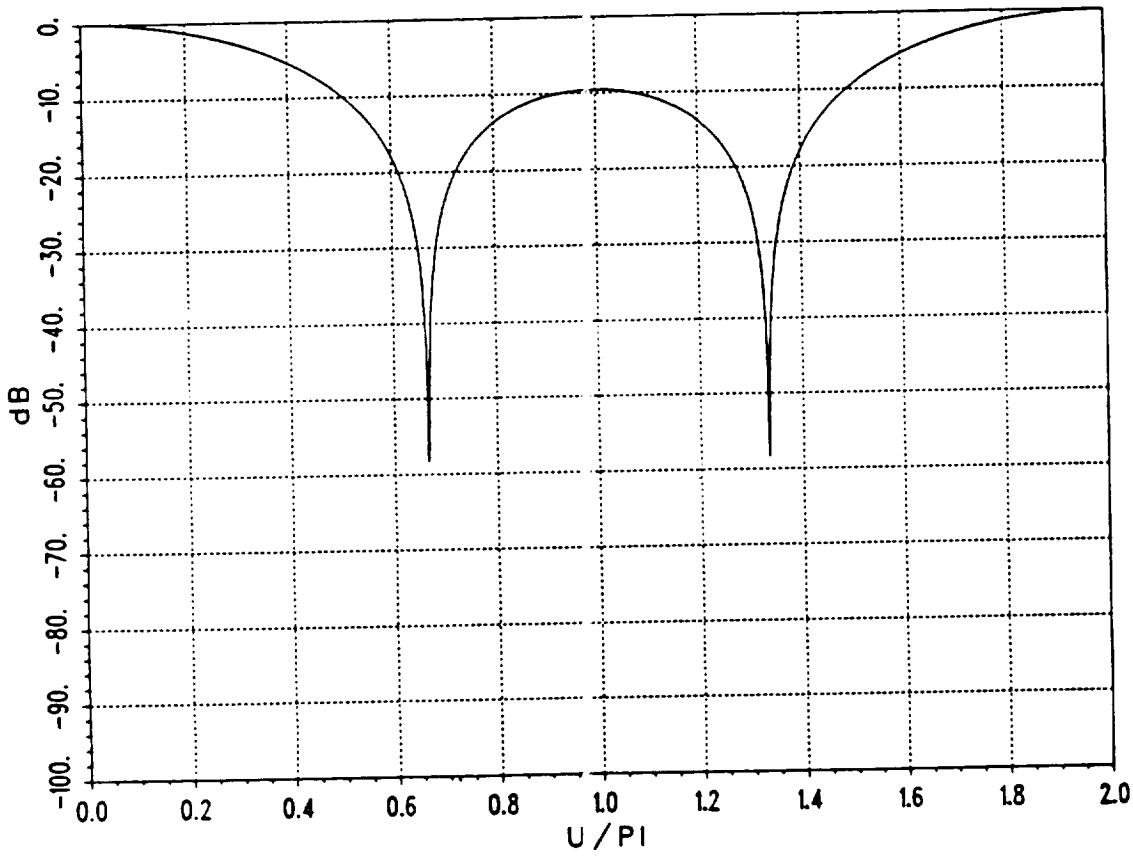

Figure 3.1. Normalized array factor for M=3.

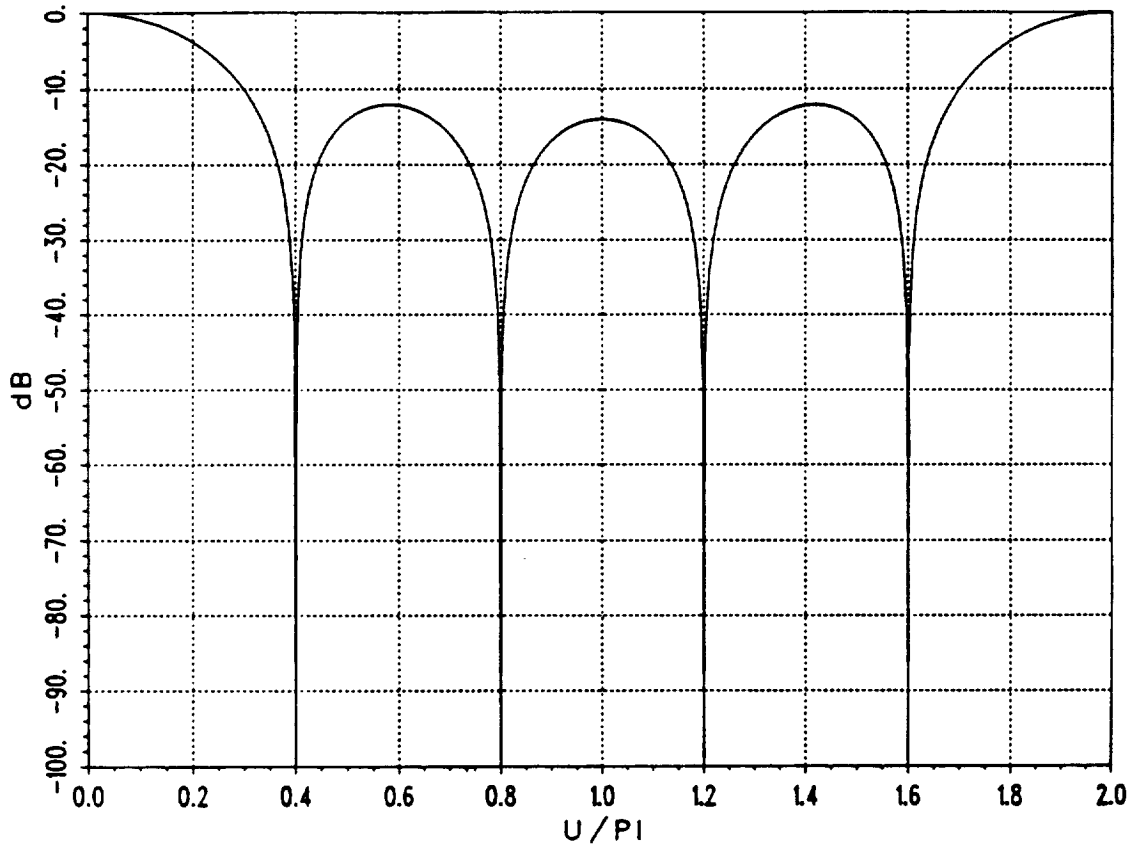

Figure 3.2. Normalized array factor for M=5.

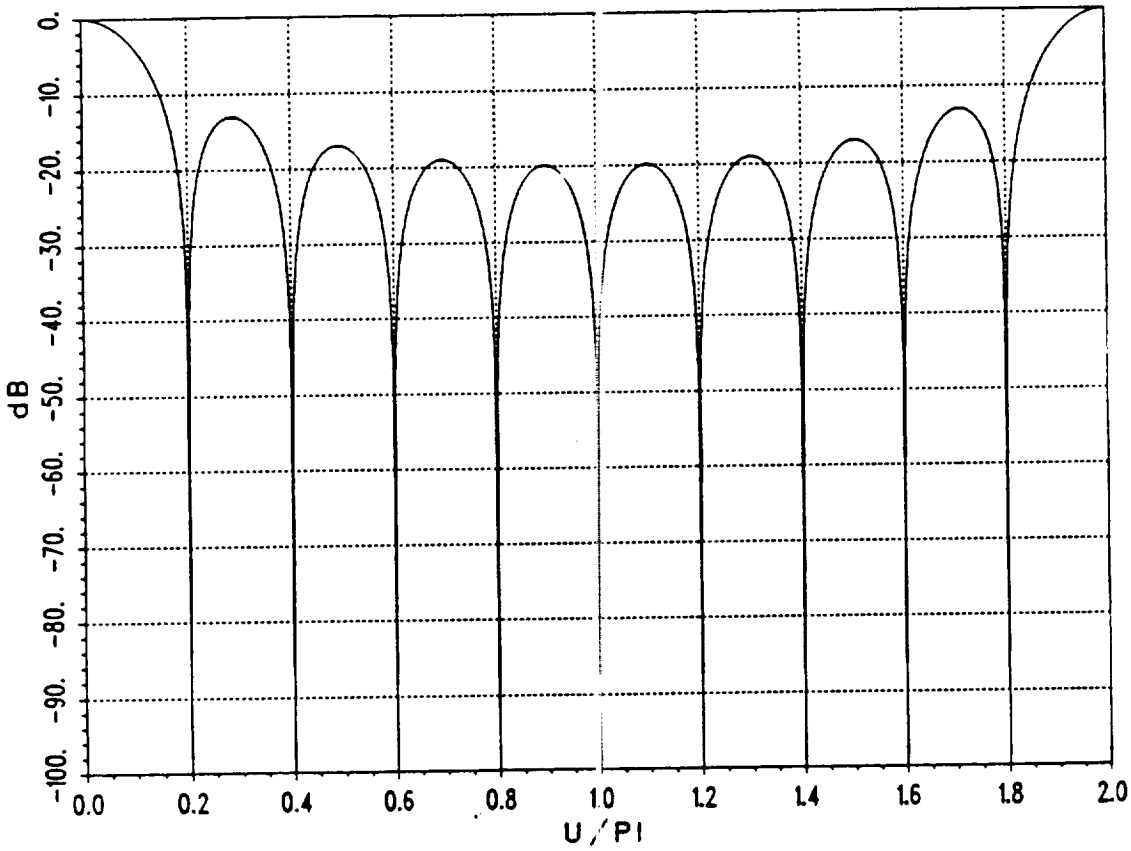

Figure 3.3. Normalized array factor for M=10.

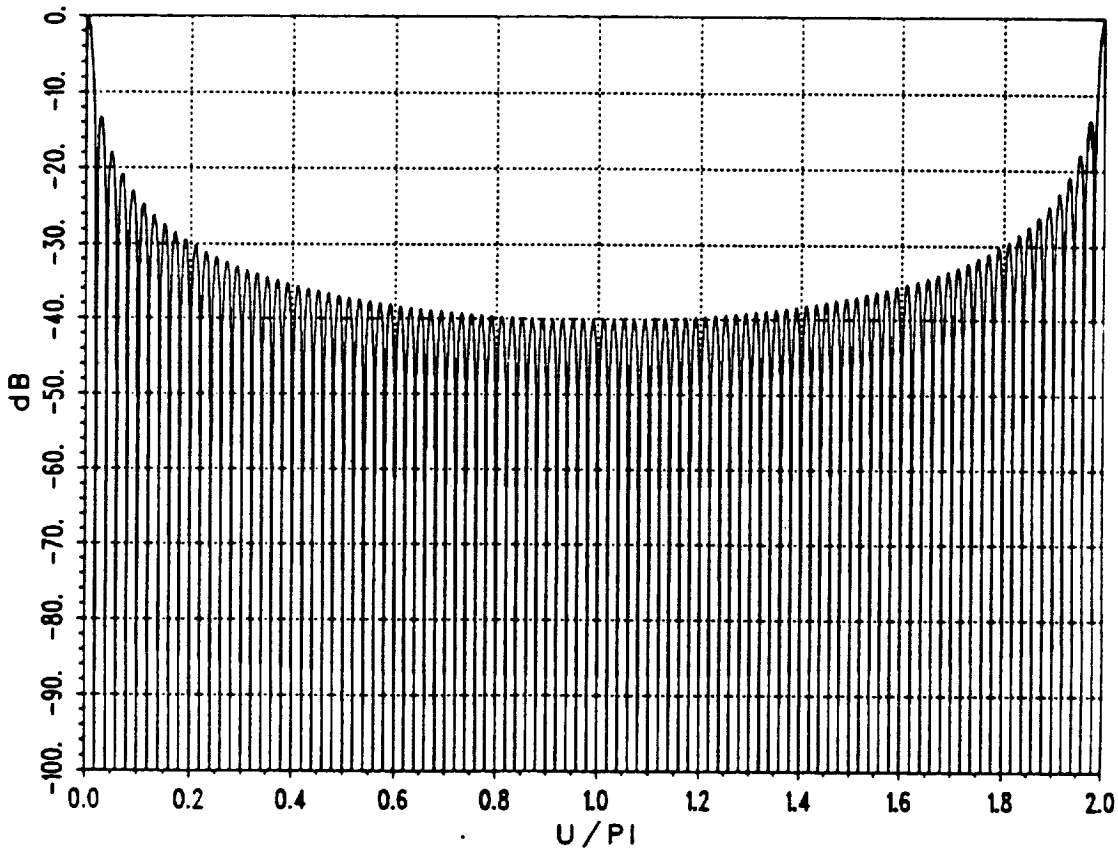

Figure 3.4. Normalized array factor for M=100.

which when compared to the boundary for an array antenna, $u_m = 2\pi\, a/2$, shows that the visible region is twice as large for the array of scatterers. From this equation, and knowing that the array factor has a period of 2π, it can be seen that more than one period will occur if

$$\frac{\Lambda}{\lambda} \geq \frac{1}{2} \quad . \tag{3.5}$$

The important consequence of this is that under this condition, the main lobe is repeated, which creates a grating lobe in the backscatter pattern. Recall that in an antenna array, a grating lobe is ensured when the element spacing is one wavelength. The fact that periods of one half wavelength cause grating lobes in a backscatter pattern is again due to the factor of two in Equation (3.3). For spatial periods that are less than a half wavelength, there is only one main lobe and only a portion of one full period of the array factor appears in real space.

The periodicity of the array factor allows the grating lobe positions to be predicted by,

$$\sin\theta = \frac{n}{2(\Lambda/\lambda)} \quad . \tag{3.6}$$

where n is an integer, up to and including the largest integer that satisfies

$$n \leq 2(\Lambda/\lambda) \quad . \tag{3.7}$$

These equations are true, independent of the number of periods of M, since M only affects the width of the main lobe, and not the position.

The array factor is an important consideration, when determining the effects of distortions on the multilayer, because of the grating lobes. Even though far out grating lobes are reduced by the cos(θ) factor in the final pattern, this factor is only -3 dB at 45°. Thus, many grating lobes could give returns on the same order of magnitude as the broadside backscatter. Further, it must be remembered that the return of a single period of distortion will have the envelope of the array factor impressed on it, in the final backscattered field. Examples of these single period returns, are given in the following sections.

C. Radar Cross Section due to Gaussian Ice Layers

In earlier work on the backscatter from layer distortions in dielectric multilayers [6], it was found that a convenient distortion function to use was the Gaussian function. The study compared results produced by the Physical Optics technique with results generated by a Moment Method technique. The results compared favorably out to about 15° away from grazing incidence. Therefore, this study will present Physical Optics results for the range of angles

$$0° \leq \theta \leq 75°.$$

Note that the backscatter pattern is symmetric about $\theta=0°$ for the geometries to be considered.

The frequency used in the examples is 10 GHz. For convenience, the period of the ice distortion function is chosen to be one wavelength at this frequency. Thus, the width of the section of the ground plane, which is beneath this ice, is 1.1803". For reference, it is instructive to examine the backscatter pattern of this section of the ground plane alone. This pattern is presented in Figure 3.5 and it applies to both TE and TM polarizations. The analysis presented in Section II seeks to determine how the ice layer changes this pattern.

The section of the ground plane is covered by a Gaussian ice layer as shown in Figure 3.6. The thickness of the ice layer is given by,

$$D(y) = \begin{cases} Ae^{-\frac{1}{2}\left(\frac{y}{\sigma}\right)^2} \text{ inch} & y \leq |\lambda/2| \\ 0 & y > |\lambda/2| \end{cases} \tag{3.8}$$

where A is the amplitude of the Gaussian function and σ is a parameter which controls the shape of the ice layer and is not the radar cross section. In the figure, B is the thickness of the ice layer at the end of the period. This thickness of ice, covering the entire section of ground plane, will be referred to as the base layer of ice. The base layer of ice, over the ground plane, is used to calculate $R_o(\theta)$ in Equations (2.29) and (2.42). This reflection coefficient is then subtracted from the reflection coefficient of the Gaussian ice layer over the ground plane to produce the subtracted backscatter pattern represented by Equations (2.29) and (2.42). Hence, the subtracted backscatter pattern represents the effect of the Gaussian ice bump on

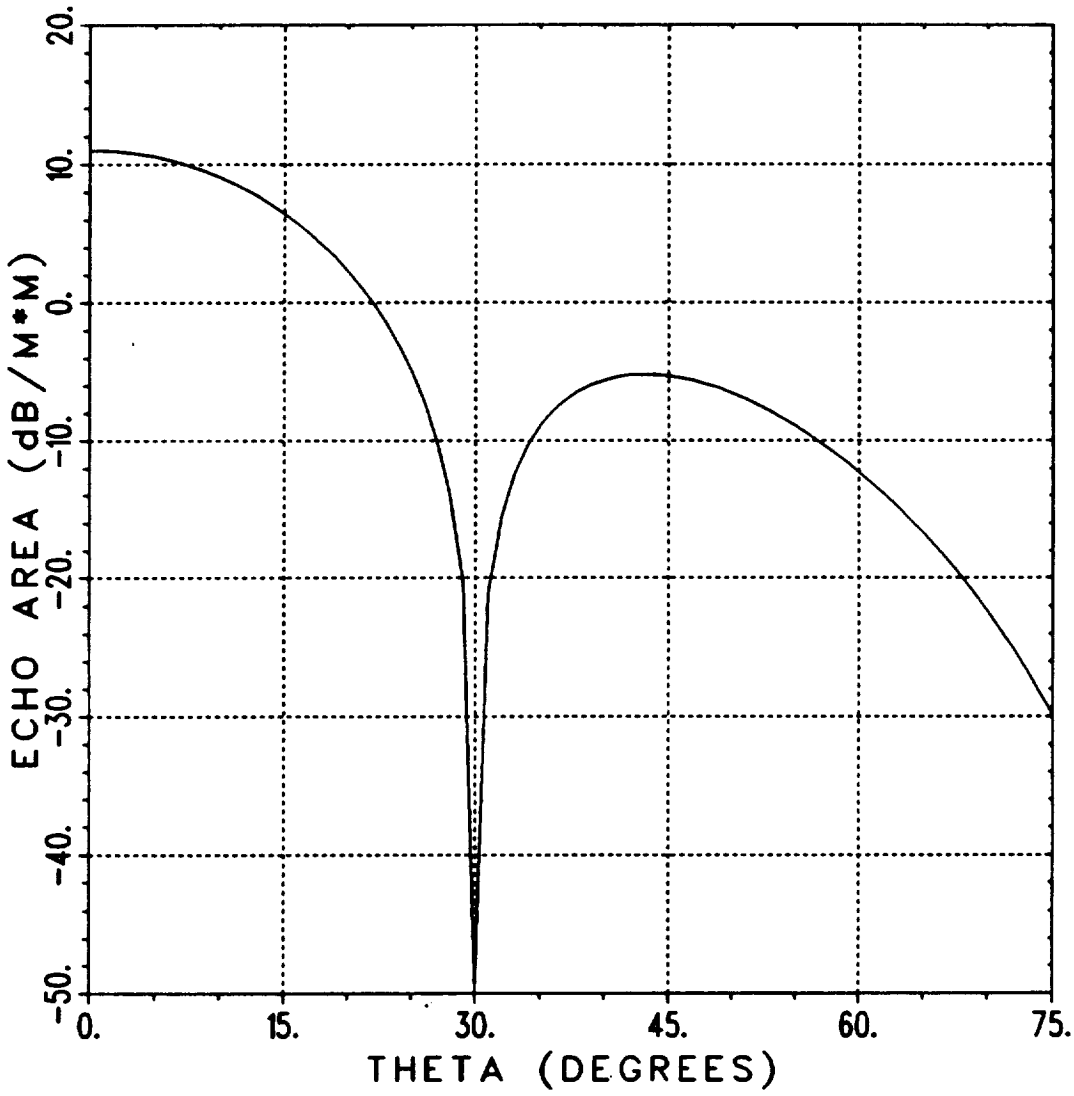

Figure 3.5. The backscatter pattern of the plate alone, L_x=1 meter, L_y=1.1803 inches and f=10 GHz.

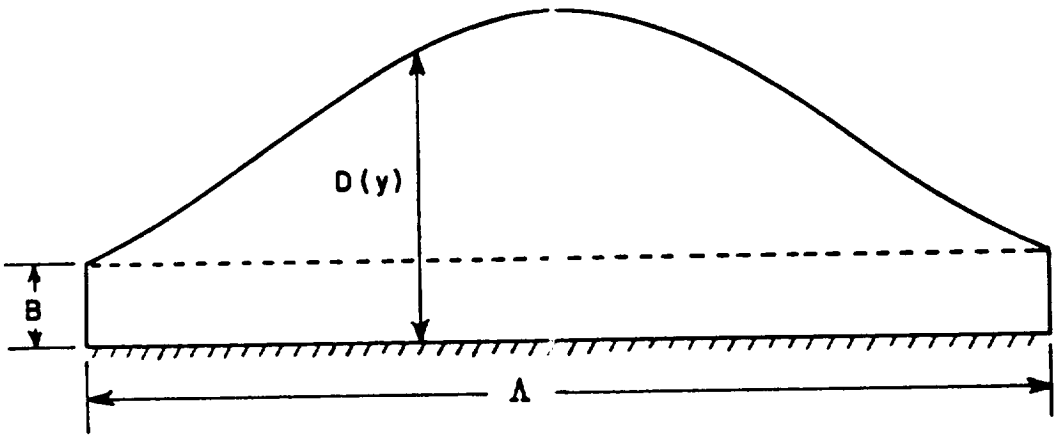

Figure 3.6. One period of a Gaussian ice layer covering a ground plane.

the backscatter pattern of the ground plane and base layer of ice. However, it will soon be shown that the base layer of ice has very little effect on the backscatter of the ground plane.

The independent parameters which are used in the examples are the amplitude of Gaussian function A, and the thickness of base layer B. The choice of these two parameters determines the value of σ which is found from,

$$\sigma = \frac{\Lambda}{2\sqrt{2\ \ln(A/B)}} \tag{3.9}$$

This equation is derived from Equation (3.8) by using

$$D(\lambda/2) = B \tag{3.10}$$

and solving for σ.

Before the subtracted backscatter patterns can be calculated, the constitutive parameters of ice must be determined. Pure water ice is non-magnetic and therefore the relative permeability is unity. The complex relative permittivity is given by [7],

$$\varepsilon_r = \varepsilon_r' - j\varepsilon_r'' \tag{3.11}$$

where

$$\varepsilon_r' = \frac{\varepsilon_1 + \varepsilon_2 \alpha^2 f^2}{1 + \alpha^2 f^2} \tag{3.12}$$

$$\varepsilon_r'' = \frac{(\varepsilon_1 - \varepsilon_2)\alpha f}{1 + \alpha^2 f^2} \tag{3.13}$$

and f is the frequency in Hz. For pure water ice,

$$\varepsilon_1 = 75$$

$$\varepsilon_2 = 3$$

$$\alpha = 1.2 \times 10^{-4}\, e^{-0.1T}\ (s)$$

where T is the temperature in degrees C. These relations are good from D.C. to 10 GHz and from 0°C to -70°C. For 10 GHz and 0°C,

$$\varepsilon_r' = 3.00$$

and

$$\varepsilon_r'' = 6.00 \times 10^{-5} \tag{3.14}$$

At 10 GHz and -70°C,

$$\varepsilon_r' = 3.00$$

and

$$\varepsilon_r'' = 5.47 \times 10^{-8} \tag{3.15}$$

Thus at 10 GHz and any applicable temperature, pure water ice is nearly lossless. Therefore, the examples will use the relative permittivity represented by Equation (3.14).

The geometry of the ice layers in the first example is represented in Figure 3.7. This example considers a base layer of 0.025 inch and four Gaussian function amplitudes with A=0.05, 0.1, 0.15 and 0.2 inch. First, consider the backscatter of the base layer over the section of the ground plane. This is shown in Figure 3.8 which is applicable to both TE and TM polarizations. Comparing this figure with the pattern in Figure 3.5 shows the negligible effect that the base layer has on the backscatter of the conducting plate

The effect of the Gaussian bumps for TE wave incidence can be seen in Figure 3.9(a). This figure shows the subtracted backscatter represented by Equation (2.29). Recall that this figure represents the changes in the backscatter pattern due to the introduction of the Gaussian ice bump on the uniform base layer. This figure indicates that

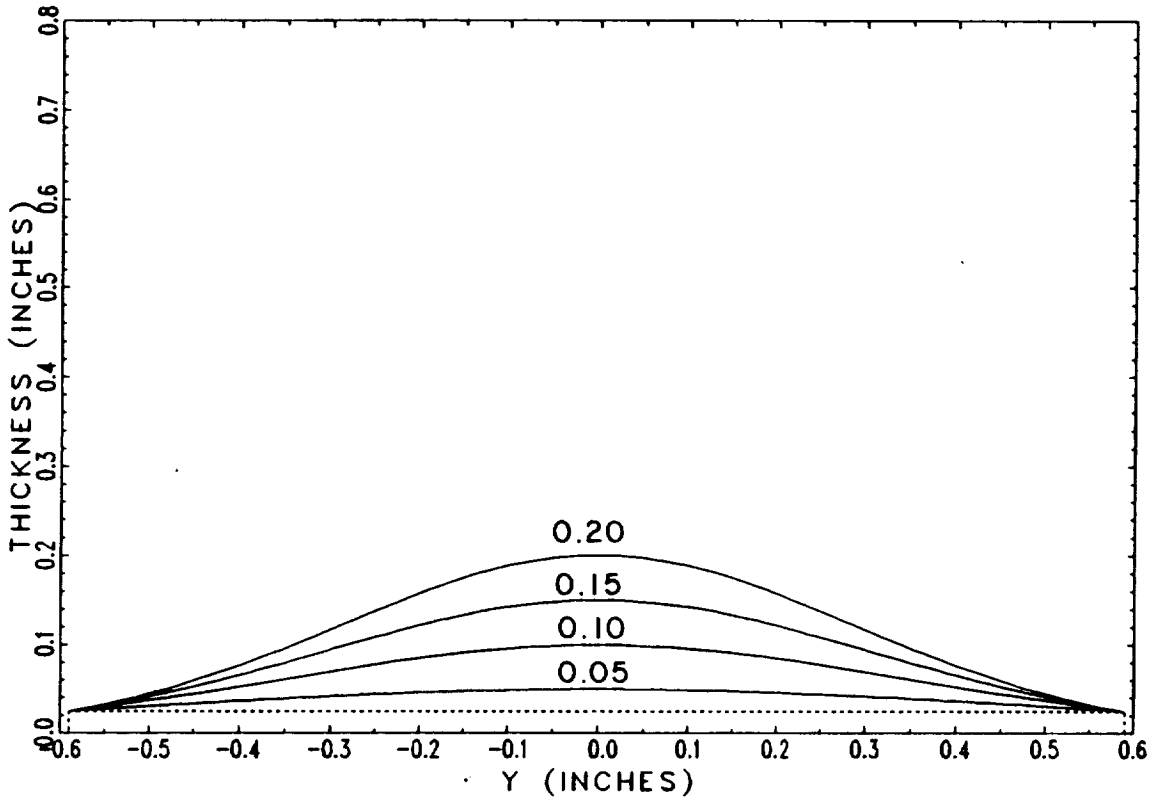

Figure 3.7. Gaussian ice layers for the first example, B=0.025 inch, A=0.05, 0.1, 0.15, 0.2 inch, f=10 GHz.

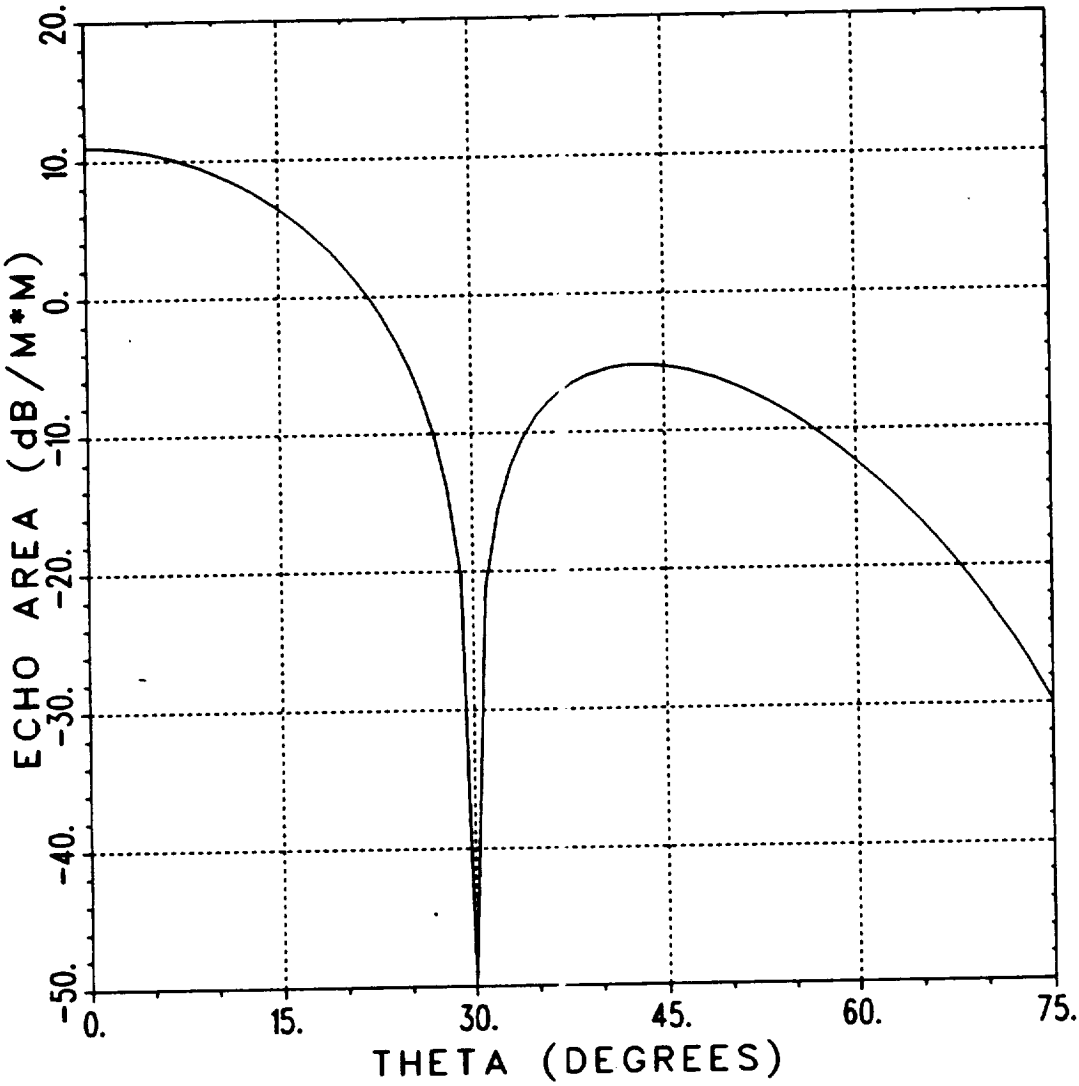

Figure 3.8. Backscatter of 0.025 inch ice base layer over a plate, L_x=1 meter, L_y=1.1803 inches and f=10 GHz.

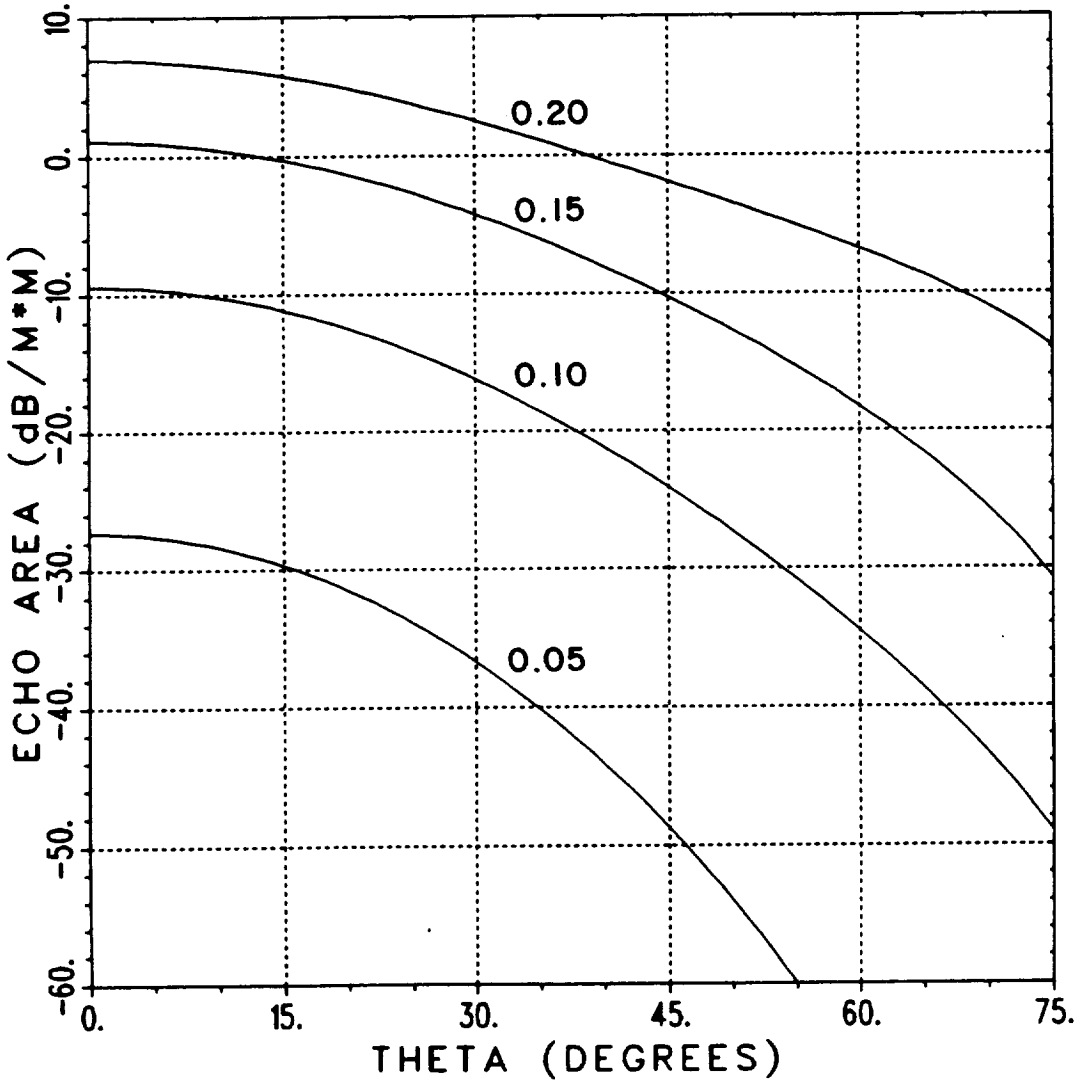

(a) TE wave incidence

Figure 3.9. Subtracted backscatter for Example 1, B=0.025 inch, A=0.05, 0.1, 0.15, 0.2 inch, L_x=1 meter, L_y=1.1803 inches and f=10 GHz.

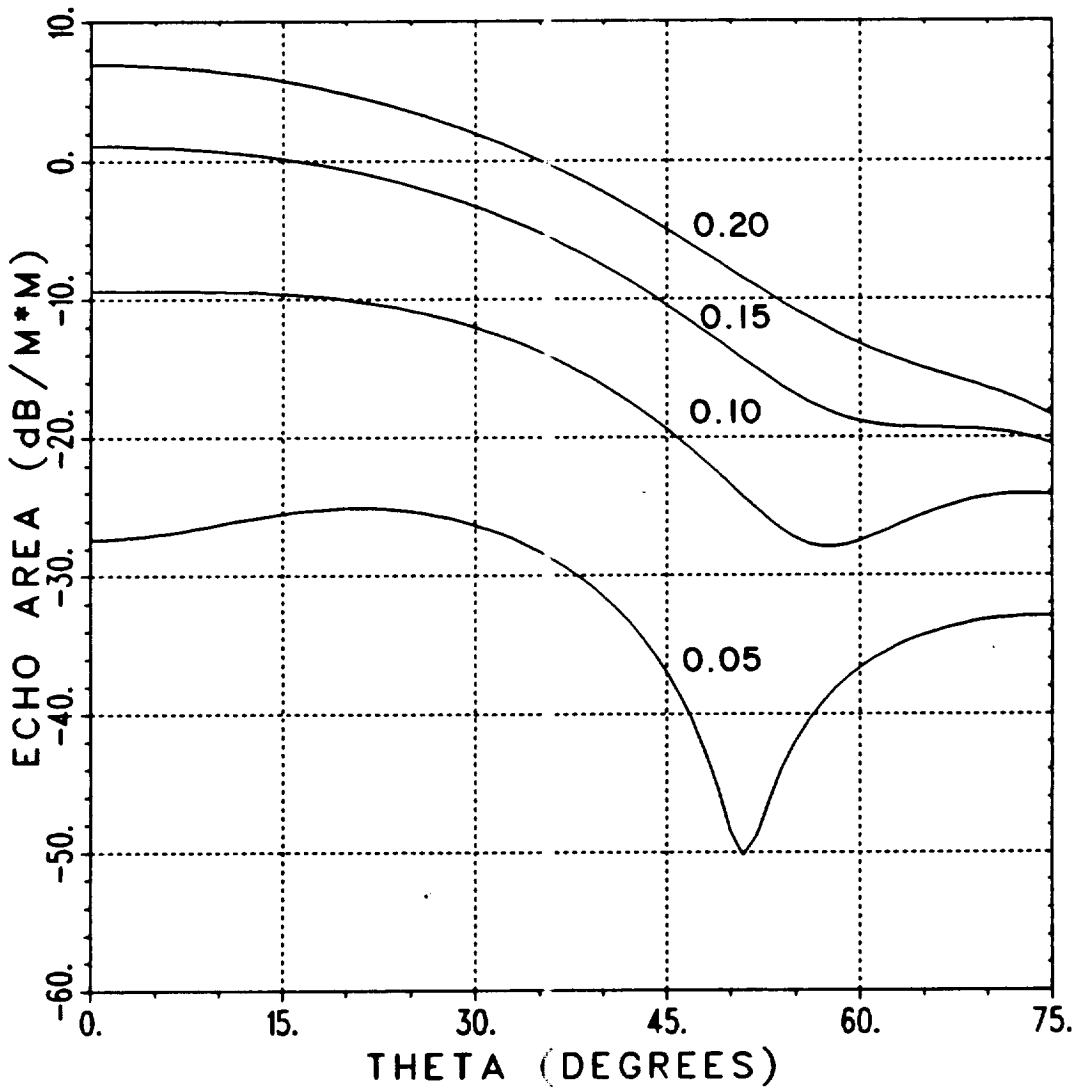

(b) TM wave incidence

Figure 3.9. Continued.

the effect is greater for thicker ice layers, at all angles. The subtracted backscatter for this example, with TM wave incidence, is shown in Figure 3.9(b). Again, the effect is greater for the thicker layers.

The limitations of the model must be kept in mind while examining the calculated results. Since the model is based on a Physical Optics approximation, the condition

$$\hat{n} \doteq \hat{z}$$

where $\hat{n}$ is the normal to the surface, must hold. This approximation becomes worse as the amplitude of the distortion is increased. Additionally, the shadowing which occurs as the incidence angle approaches grazing is not included in the analysis.

The geometry of the ice layers considered in the second example is shown in Figure 3.10. Here a base layer of 0.05 inch thickness is used along with Gaussian function amplitudes of A=0.1, 0.15 and 0.2 inch. The backscatter of the base layer, backed by the conducting plate is shown in Figure 3.11. Again the nearly lossless ice has negligible effect on the backscatter of the plate. The subtracted backscatter for this example is shown in Figure 3.12. The trend of an increased backscatter level, for thicker ice layers, is exhibited in these calculations also.

The geometry of the ice layers considered in the third example is shown in Figure 3.13. Here a base layer of 0.10 inch is used along with Gaussian function amplitudes of A=0.15 and 0.2 inch.

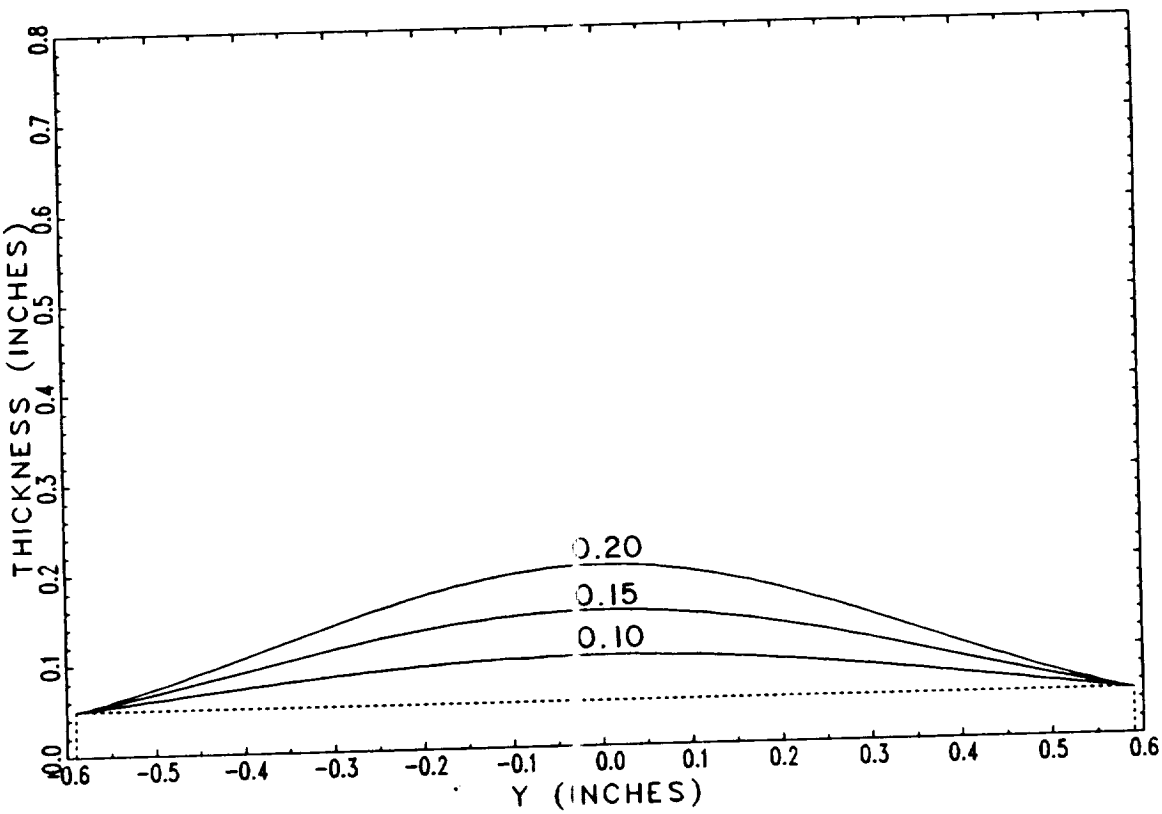

Figure 3.10. Gaussian ice layers for the second example, B=0.05 inch, A=0.1, 0.15, 0.2 inch, f=10 GHz.

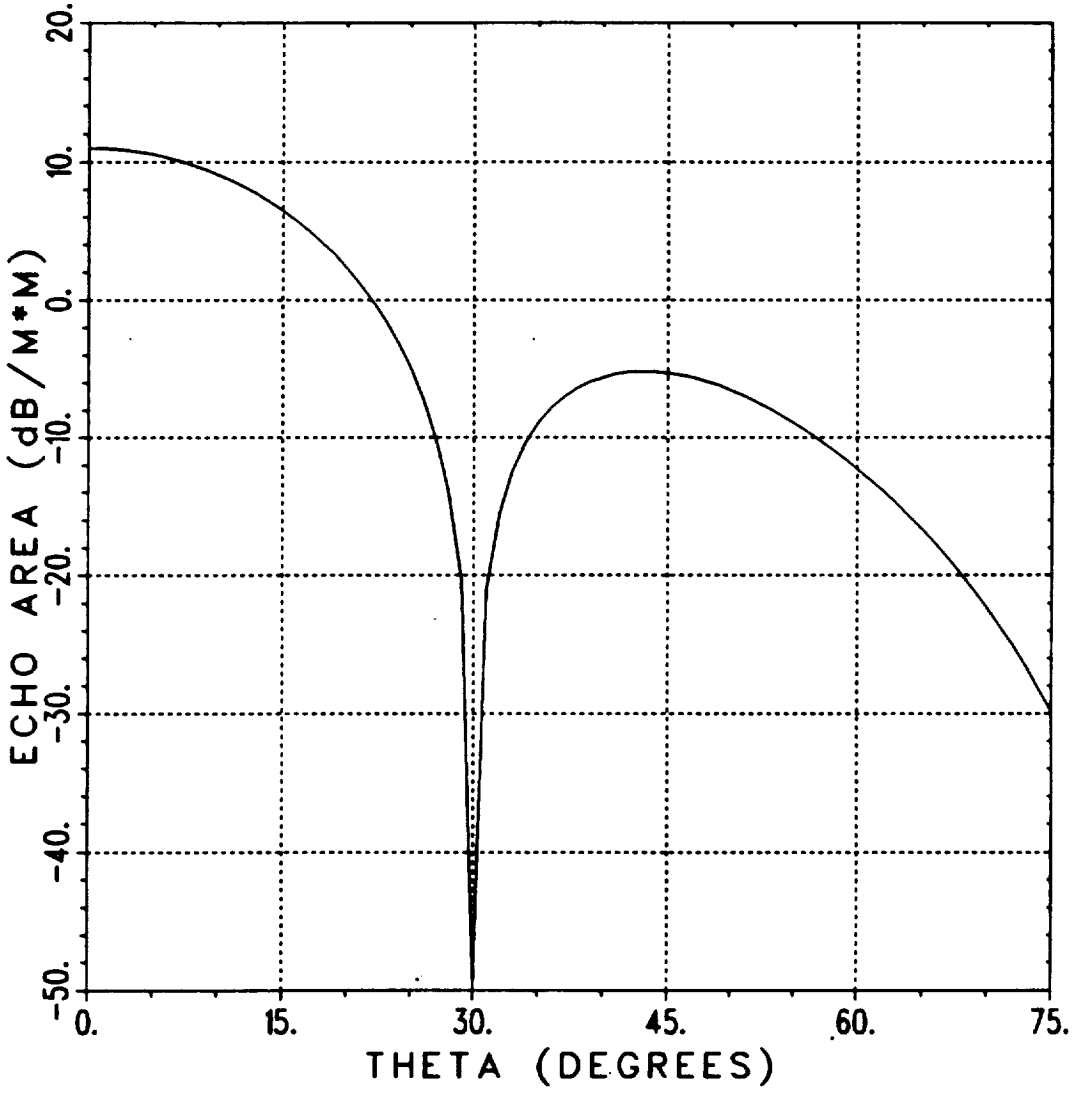

Figure 3.11. Backscatter of 0.05 inch layer over a plate, L_x=1 meter, L_y=1.1803 inches and f=10 GHz.

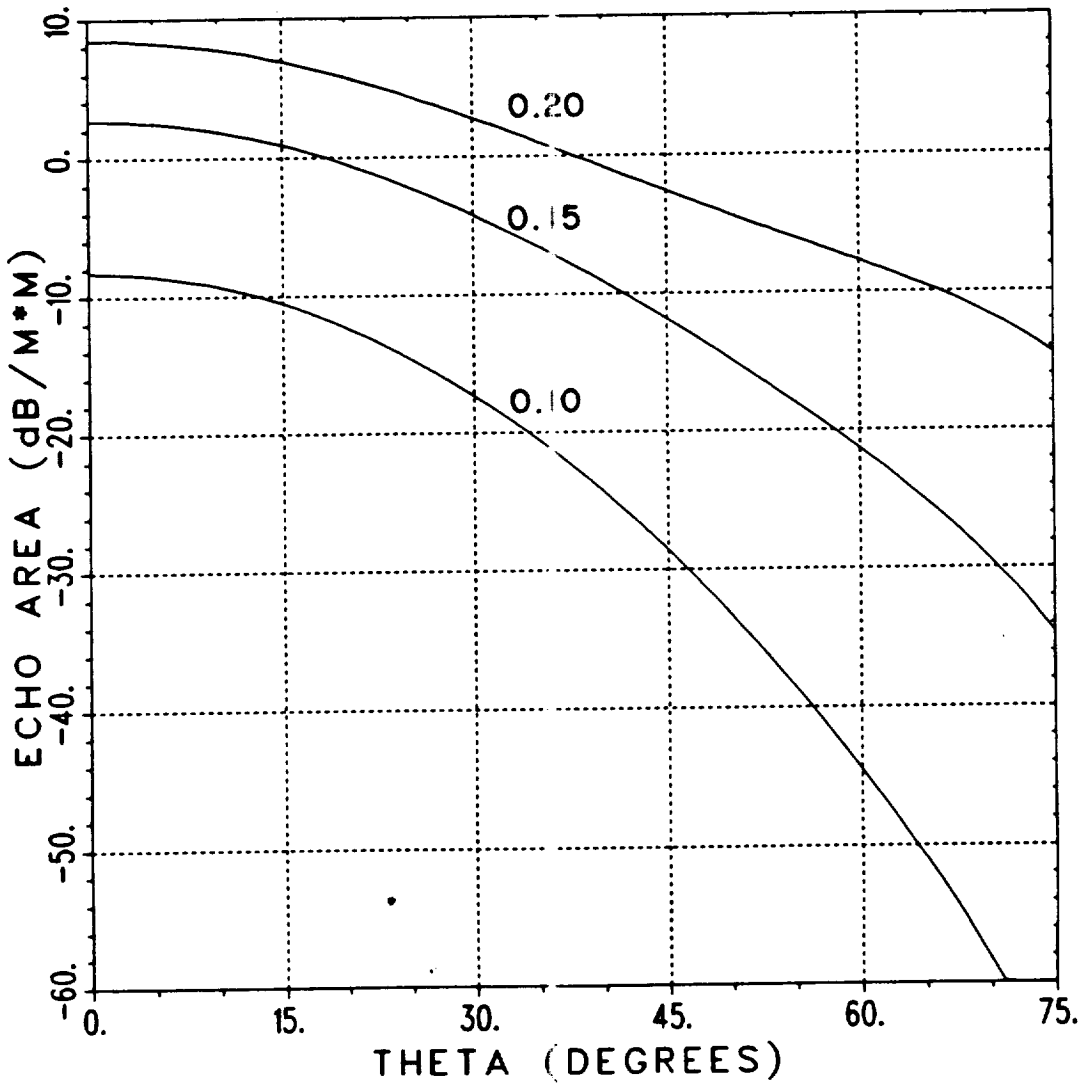

(a) TE wave incidence

Figure 3.12. Subtracted backscatter for Example 2, B=0.05 inch, A=0.1, 0.15, 0.2 inch, L_x= 1 meter, L_y=1.1803 inches and f=10 GHz.

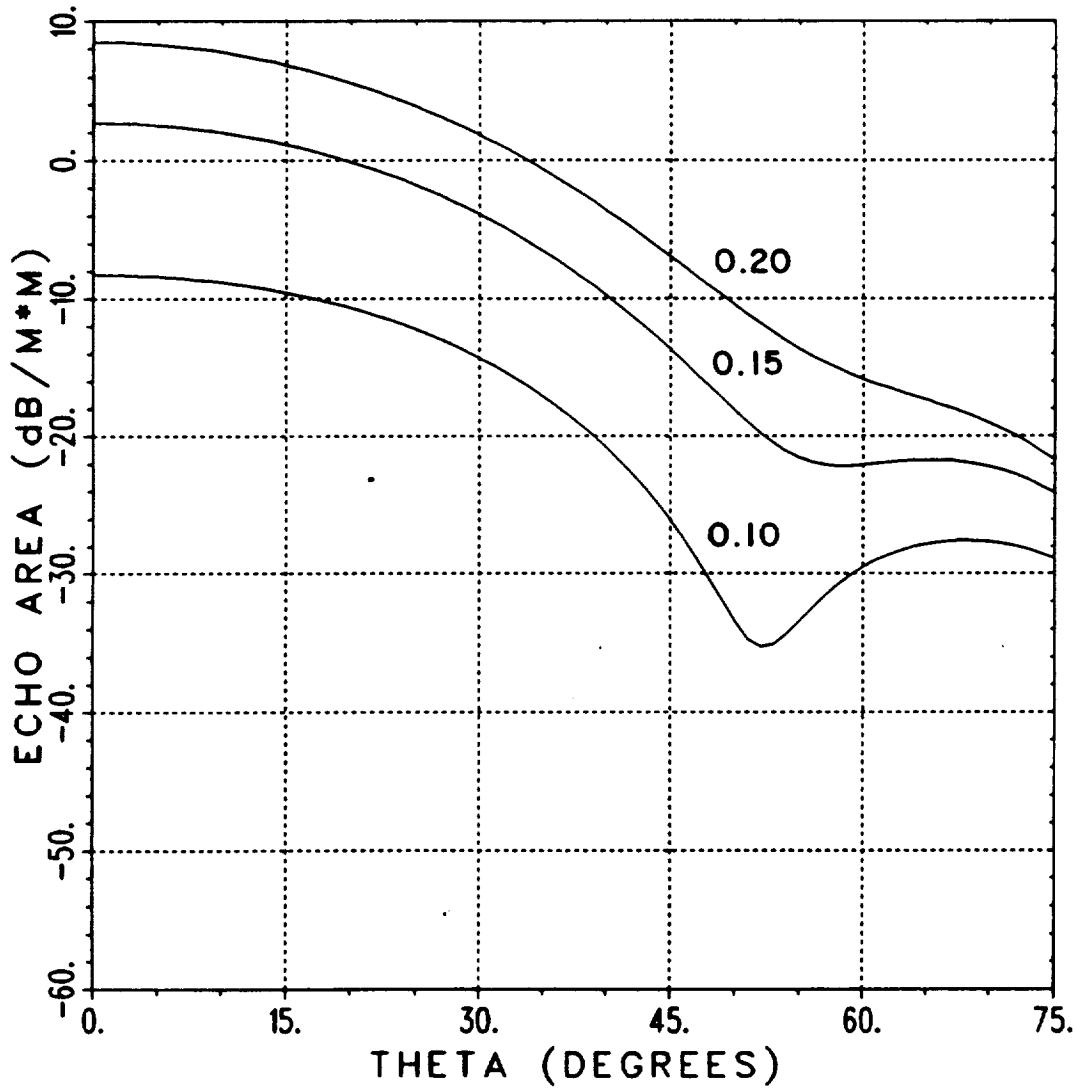

(b) TM wave incidence

Figure 3.12. Continued.

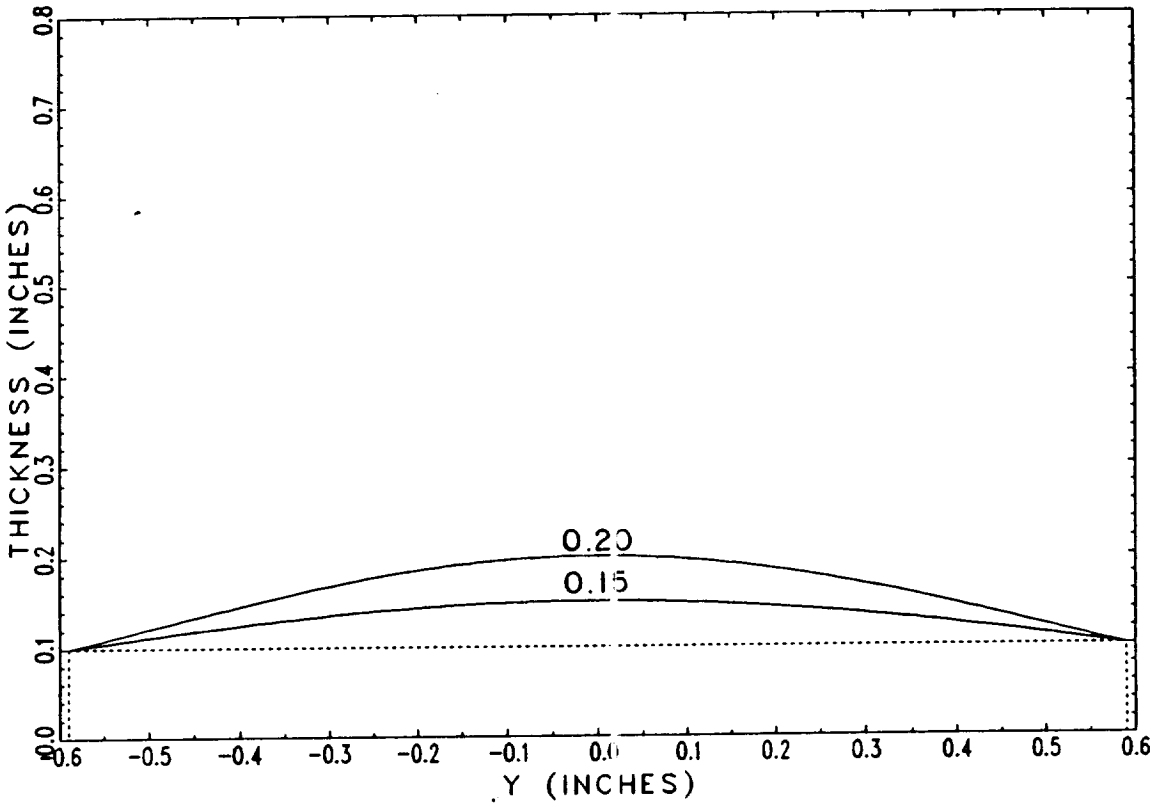

Figure 3.13. Gaussian ice layers for the third example, B=0.1 inch, A=0.15, 0.2 inch, f=10 GHz.

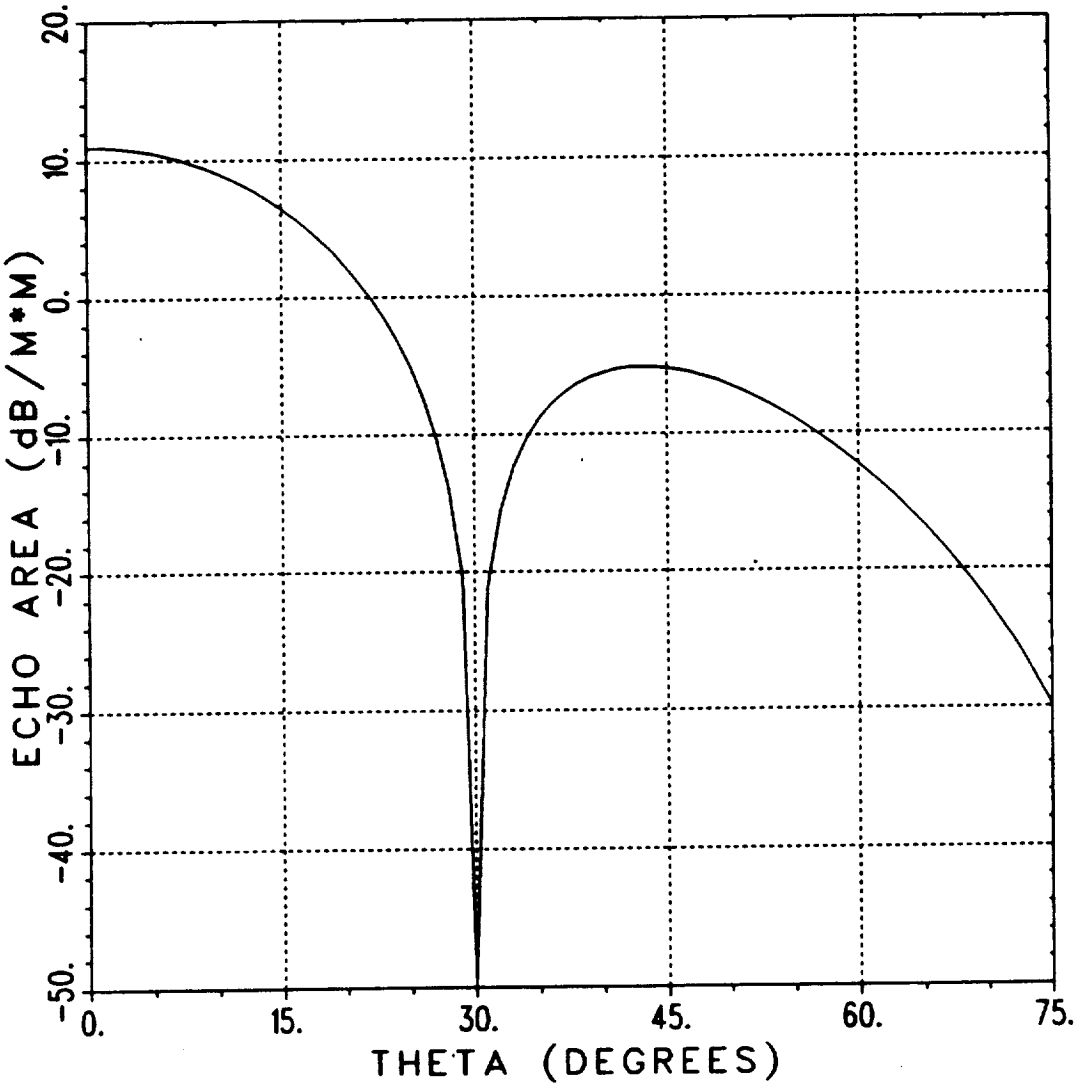

Figure 3.14. Backscatter of 0.10" base layer over a plate, L_x=1 meter, L_y=1.1803 inches and f=10 GHz.

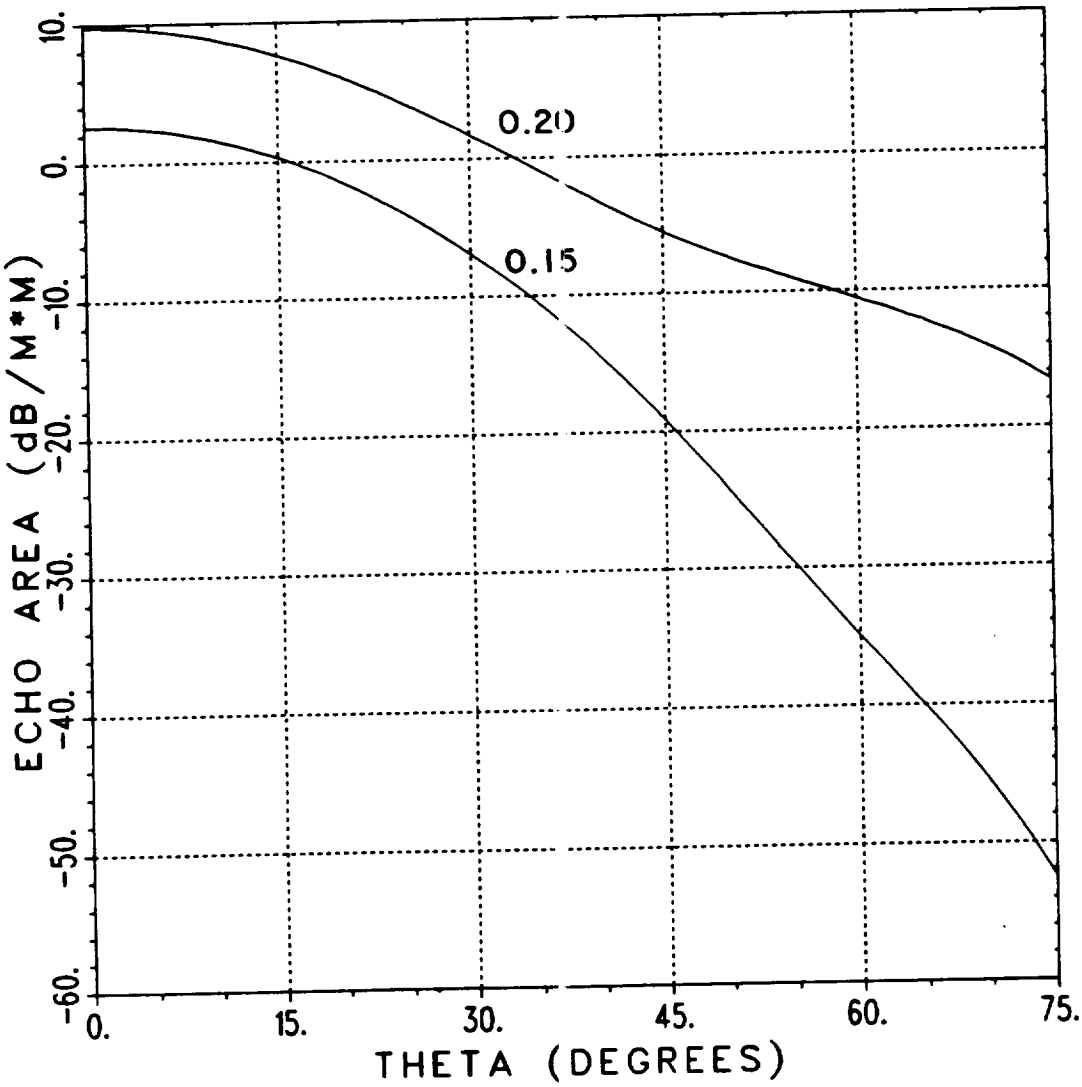

(a) TE wave incidence

Figure 3.15. Subtracted backscatter for Example 3, B=0.10 inch, A=0.15, 0.2 inch, L_x=1 meter, L_y=1.1803 inches and f=10 GHz.

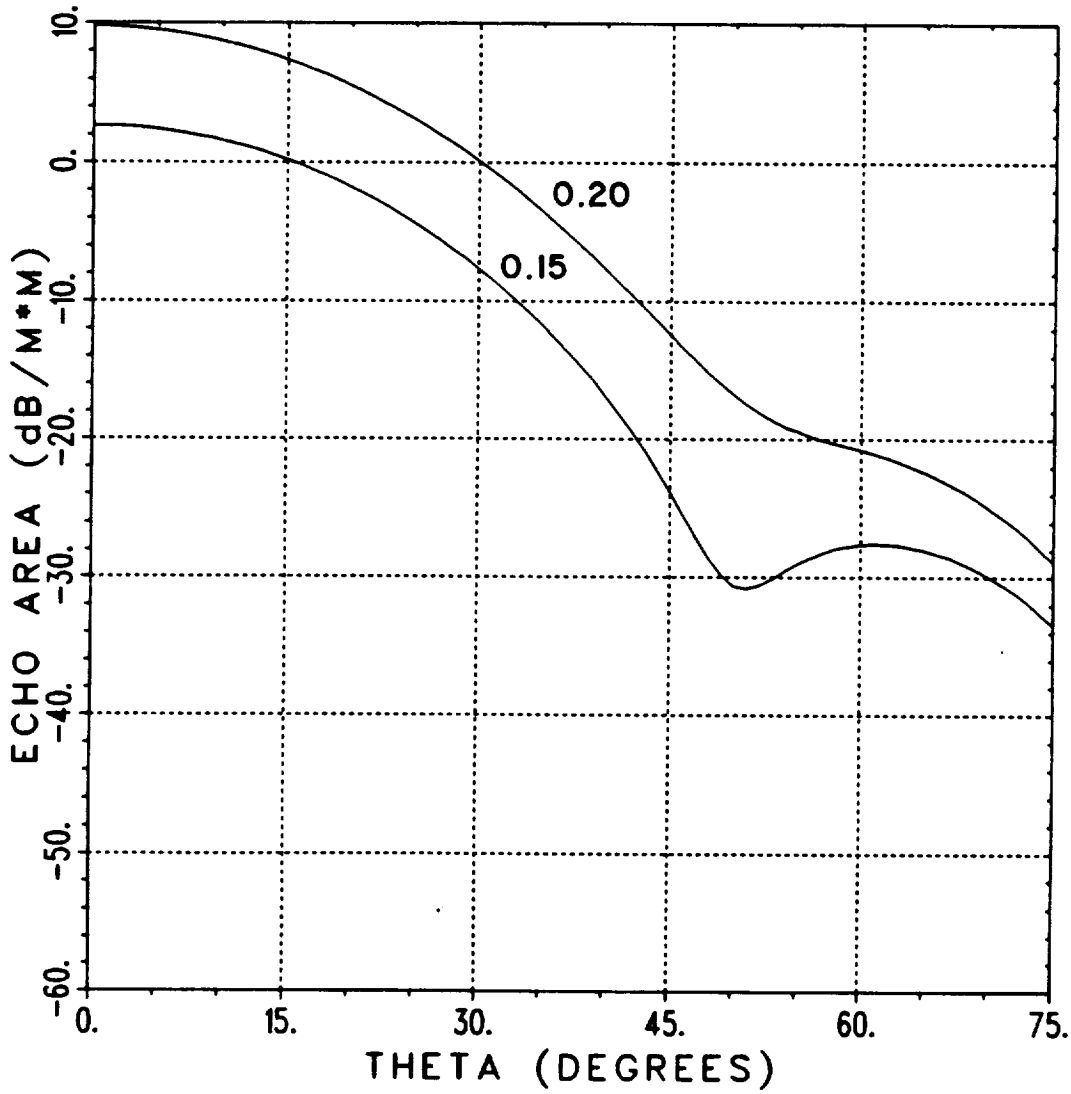

(b) TM wave incidence

Figure 3.15. Continued.

The backscatter of the base layer, backed by the conducting plate, is shown in Figure 3.14. Comparison of Figure 3.14 with Figure 3.5 shows that the base layer has negligible effect on the backscatter of the plate. The subtracted backscatter for this example is shown in Figure 3.15. Again, a greater thickness of ice causes a greater effect on the backscatter of the plate.

The reason that the subtracted backscatter levels increase with an increase in the thickness of the ice layer is related to the fact that the ice is nearly lossless. Because the ice is nearly lossless, the thickness of the layer only modifies the phase of the reflection coefficient. The modification to the magnitude of the reflection coefficient is negligible. This was demonstrated in Figures 3.8, 3.11 and 3.14, which showed that a base layer of ice does not significantly effect the backscatter pattern of the plate. Again we observe that this is dependent on satisfying the approximation that $\hat{n} \doteq \hat{z}$ since the reflection (transmission) coefficient at the first interface becomes dependent on the incidence angle.

D. Summary

In this chapter, the practical implications of the results derived in Section II were considered. These derivations show that a periodic ice cover over a ground plane may be treated as an array of individual scatterers. Each element in this array is a section of the ground plane, covered by one period of the ice layer. The backscattered field of the array is the product of the individual response of a single

element and an array factor which takes into account the phase differences between the elements of the array.

The first part of this section examined the array factor. The properties of the array factor were listed and the differences between an array antenna and an array of scatterers were pointed out. It was also shown that distortion periods greater than $\lambda/2$ will produce grating lobes in the backscatter pattern. Several examples of the array factor, for different numbers of elements, were given.

The response of a single period of a Gaussian ice layer over the ground plane was also examined in this section. To do this, three base layers, each with five separate thickness Gaussian functions, were considered. The results presented showed the response as a function of the amplitude of the Gaussian function and the thickness of the base layer.

IV. SUMMARY AND CONCLUSIONS

The analysis used in this report is based on an approximation so that all internal reflections can be incorporated readily into the solution. This seriously restricts the height of the ice discontinuity. To extend this analysis, it would be necessary to incorporate a ray tracing procedure to find the total reflected fields in aperture plane and proceed as before. An alternate solution would consist of using the more time consuming integral equation solution. However, it is clear for even these small height irregularities that this surface roughness is a significant contributor to the RCS. It will only increase as the height is increased.

This report has investigated the effect of variations in the thickness of an ice layer on the backscattered field of a ground plane.

When the variation is periodic, it has been found that the structure may be treated as an array of scatterers, with the elements of the array being a section of the ice covered ground plane, containing a period of the variation. The results of an individual scatterer are easily extended to a structure containing many such scatterers. Several examples were given to show the response from ice layers having a Gaussian shape.

The scattering analysis presented in this report is based on a Physical Optics approximation. Therefore, it is anticipated that the analysis is the most accurate for angles of incidence near broadside. As the angle of incidence approaches grazing, the Physical Optics approximation is not an adequate representation of the true scattering mechanisms. Additionally, the accuracy of the Physical Optics approximation depends on the type of distortion function being considered. The amplitude and period of the distortion function must be such that the radius of curvature is sufficiently large to allow this to be a reasonable approximation. Earlier comparisons of the results of the Physical Optics technique with Moment Method calculations indicate that the Physical Optics technique should give reasonable results to within 15° of grazing incidence [6].

Finally, it should be noted that the amplitudes of the distortion function chosen for use in the examples, were an arbitrary choice. It is possible that the value chosen may not be typical of what occurs in practice. Therefore it is likely that the examples with the largest amplitudes should be treated as worst cases.

REFERENCES

[1] K.M. Lambert and L. Peters, Jr., "An Investigation into a Class of Layer Distortions in Dielectric Multilayers," Report No. 720314-2, The Ohio State University ElectroScience Laboratory, prepared under Contract No. L7EN-10719-175 for Rockwell International Corporation, Los Angeles, CA, January 1988.

[2] R.F. Harrington, Time Harmonic Electromagnetic Fields, Section 3-13, New York: McGraw-Hill, 1961.

[3] J.H. Richmond, "Efficient Recursive Solutions for Plane and Cylindrical Multilayers," Technical Report RF1968-1, The Ohio State University ElectroScience Laboratory, generated under Contract No. NOw 65-0329-d, for Bureau of Naval Weapons, Washington, D.C., August 1965.

[4] W.L. Stutzman and G.A. Thiele, Antenna Theory and Design, p. 125, New York: John Wiley & Sons, 1981.

[5] J.D. Kraus, Antennas, Appendix 17, McGraw-Hill, New York, 1950.

[6] K.M. Lambert and L. Peters, Jr., "Moment Method Calculation of the Backscatter Due to Layer Distortions in Dielectric Multilayers," Report No. 720314-4, The Ohio State University ElectroScience Laboratory, prepared under Contract No. L7EN-10719-175, for Rockwell International Corporation, Los Angeles, CA, June 1988.

[7] E.R. Pounder, Physics of Ice, p. 129, Pergamon Press, New York, 1965.